Based on Network Pharmacology to Explore the Molecular Mechanism of Buzhong Yiqi Decoction for the Treatment of Gastric Cancer

Ruiping Yang
Hubei University of Chinese Medicine
Xiaojing Lin
Hubei University of Chinese Medicine
Chunhui Tao
Hubei University of Chinese Medicine
Ruixue Jiang (349313205@qq.com)
Hubei University of Chinese Medicine

Research Article

Keywords: Buzhong Yiqi Decoction, Gastric cancer, Network pharmacology, Molecular docking, Molecular dynamics simulation

Posted Date: November 30th, 2021

DOI: https://doi.org/10.21203/rs.3.rs-1098024/v1

Abstract

Background

Buzhong Yiqi Decoction (BZYQD) has been widely accepted as an alternative treatment for gastric cancer (GC) in China. The present study set out to determine the potential molecular mechanism of BZYQD in the treatment of GC by means of network pharmacology, molecular docking, and molecular dynamics simulation.

Methods

The potential active ingredients and targets of BZYQD were screened out through the Traditional Chinese Medicine Systems Pharmacology (TCMSP). GC-related targets were screened out through the GeneCards database, and the intersection targets of BZYQD and GC were obtained by using the Venn diagram online tool. Then, the TCM-Active Ingredient-Target network was constructed by using the Cytoscape, and the protein-protein interaction (PPI) network was constructed by using the STRING database. Gene Ontology (GO) and Kyoto Encyclopedia of Genes and Genomes (KEGG) enrichment analyses of the effective targets of BZYQD in GC were performed through the Metascape platform. Finally, the molecular docking between the compounds and the target proteins was performed by using the AutoDock Vina software. The simulation of molecular dynamics was conducted for the optimal protein-ligand complex obtained by molecular docking using the Amber18 software.

Results

A total of 150 active ingredients of BZYQD were retrieved, corresponding to 136 targets of GC. The key active ingredients were quercetin, kaempferol, nobiletin, naringenin, and formononetin. The core targets were AKT1, STAT3, TP53, MAPK1, and MAPK3. GO functional enrichment analysis showed that BZYQD treated GC by affecting various biological processes such as oxidative stress, chemical stress, lipopolysaccharide reaction, and apoptosis. KEGG pathway enrichment analysis indicated that the apoptosis signaling pathway, PI3K/Akt signaling pathway, proteoglycan in cancer, IL-17 signaling pathway, TNF signaling pathway, and HIF-1 signaling pathway were involved. Molecular docking results revealed the highest binding energy for MAPK3 and naringenin. The stable binding of MAPK3 and naringenin was also demonstrated in the molecular dynamics simulation test, with the binding free energy of -25kcal/mol.

Conclusion

This study preliminarily revealed the multi-component, multi-target, and multi-pathway characteristics of BZYQD against GC, laying a scientific basis for further research on the molecular mechanism of BZYQD.

1. Introduction

Gastric cancer (GC) represents the most prevalent gastrointestinal malignant tumor worldwide, with its ever-increasing prevalence being very alarming. According to the statistics released in 2021, the morbidity of GC ranks fifth and the mortality ranks fourth in the global malignant tumors, causing more than 1 million new cases and 769,000 deaths in 2020[1]. At present, the pathogenesis of GC has not been thoroughly elucidated. The existing knowledge indicates that bacteria (such as Helicobacter pylori), smoking, and inherited mutations of specific genes (such as CDH1 gene) may underlie the prominent risk factors for GC[2]. Currently, surgical resection remains the preferred therapeutic method for GC patients, but unfortunately, the majority of GC patients have already progressed into the middle and advanced stages when they are diagnosed, with a 5-year survival rate of less than 30%[3]. Moreover, chemotherapy often elicits gastrointestinal adverse reactions and bone marrow suppression[4]. Against this backdrop, it is of great clinical significance to seek alternative or adjuvant treatment methods with few side effects and favorable curative efficacy for GC patients.

Traditional Chinese medicine (TCM) has been practiced for thousands of years in China. Accumulating studies have demonstrated that TCM combined with modern medicine can enhance efficacy and reduce toxicity in the treatment of human malignancies[5]. Buzhong Yiqi Decoction (BZYQD) is derived from the "Spleen and Stomach Theory" written by Li Dongyuan, a famous doctor in the Jin Dynasty. BZYQD is composed of 8 kinds of herbs: Astragalus membranaceus (“Huangqi” in Chinese), Atractylodes macrocephala (“Baizhu” in Chinese), Ginseng (“Renshen” in Chinese), Licorice (“Gancao” in Chinese), Tangerine Peel (“Chenpi” in Chinese), Radix bupleuri (“Chaihu” in Chinese), Angelica sinensis (“Danggui” in Chinese), and Cimicifugae (“Shengma” in Chinese). In recent years, many scholars have unveiled the great implication of BZYQD in the adjuvant treatment of GC, which contributes to reducing side effects, improving quality of life, and prolonging survival. BZYQD can restore impaired immune function, enhance the viability of natural killer cells, and exercise notable anti-tumor effects[6]. Also, BZYQD can inhibit the expression of PD-L1 via the PI3K/AKT pathway, repress the increase of CD8+PD-1+T cells in GC patients induced by chemotherapy, improve immune function, enhance tumor lymphocyte infiltration, and impede the progression of GC[7]. Yu et al.[8]have revealed that BZYQD combined with cisplatin in the treatment of malignant tumors can reverse cisplatin resistance by inducing the accumulation of reactive oxygen species (ROS), and ROS accumulation is known to activate apoptosis and autophagy through oxidative stress. Pei et al.[9]have suggested that BZYQD can improve the immune function of GC patients, facilitate the Th1/Th2 immune imbalance, and reduce the adverse reactions of chemotherapy.

Network pharmacology, an emerging discipline based on system biology and computer technology, has been extensively applied in the research field of TCM compounds in recent years due to its functionality of predicting effective ingredients, targets, toxic, and side effects of drugs[10, 11]. Therefore, this study set out to screen out the active components of BZYQD in the treatment GC and predict the related targets and signaling pathways with the support of the network pharmacology to explore the mechanism of action of BZYQD in the treatment of GC. The detailed flowchart of the present study is shown in Figure 1.

2. Materials And Methods

2.1 Screening of active ingredients and targets of BZYQD.

In line with the selection criteria of oral bioavailability (OB) ≥ 30% and drug-likeness (DL) ≥ 0.18, the active ingredients of 8 herbs in BZYQD were searched in the Traditional Chinese Medicine Systems Pharmacology (TCMSP)[12] (https://tcmspw.com/tcmsp.php), and then the targets corresponding to each active ingredient was searched. Finally, the collected target names were converted into the ID names of the corresponding genes by using the Uniport protein database[13].

2.2 Prediction of the potential targets of BZYQD in the treatment of GC.

With "gastric cancer" as the keyword and Score > 10 as the screening criteria, GC-related targets were retrieved from the GeneCards database[14]. The targets of BZYQD and the targets of GC were analyzed by using the Venn diagram online tool, and a Venn diagram was made. The intersection between the two groups of targets was considered the potential targets of BZYQD against GC.

2.3 Construction of a "TCM-Active Ingredient-Target" network.

The potential targets of BZYQD in the treatment of GC and the corresponding active ingredients were imported into Cytoscape 3.8.0[15] to construct a "TCM-Active Ingredient-Target" network to clarify the pharmacological mechanism of BZYQD against GC. The degree value reflected the importance of the node in the network. The higher the degree value, the more important the node. The key active ingredients were screened out according to the degree value.

2.4 Construction of protein-protein interaction (PPI) network and cluster analysis.

The target proteins corresponding to the components of BZYQD in GC were imported into the STRING[16] (https://string-db.org) to perform PPI analysis, with the species set to “Homo sapiens”, the confidence set to > 0.9, and unconnected nodes hidden. Then, the tsv file of PPI analysis results was imported into Cytoscape to construct a PPI network. Some target proteins had the same or similar characteristics and functions in cell biological activities, and these target proteins were regarded as a cluster. Proteins in the same cluster are generally thought to play a synergistic role in disease progression[17]. Cluster analysis of target proteins in the bioinformatics network was performed by using the MECODE plug-in of Cytoscape.

2.5 Enrichment analysis.

The Metascape platform[18] was used to perform Gene Ontology (GO) functional enrichment analysis and Kyoto Encyclopedia of Genes and Genomes (KEGG) pathway enrichment analysis on the intersection targets of BZYQD and GC. The results of enrichment analysis were saved and finally visualized by using R software. The biological process (BP), cell component (CC), and molecular function (MF) results of GO enrichment analysis were drawn into bar graphs, and the KEGG pathway enrichment analysis results were

drawn into a bubble chart for the further exploration of the biological processes and metabolic pathways of BZYQD in GC.

2.6 Molecular docking.

The top five components in degree value in the "TCM-Active Ingredient-Target" network were molecularly docked with the top five core target proteins in degree value in the PPI network. The structure of the compounds was obtained from the PubChem database[19] and the structure of the proteins was from the RCSB PDB database[20]. Then, the AutoDock software was used for molecular docking. Three conformations with the best docking binding energy were selected for the docking binding mode analysis. Discovery Studio Visualizer 2019 software was used for force analysis and PyMOL software was used for mapping.

2.7 Molecular dynamics simulation.

The amber18 software[21] was used to perform molecular dynamics simulation on the protein(target)and small molecule ligand (compound) obtained by molecular docking. FF144SB and general Amber force field (GAFF) parameters were used for proteins and small molecule ligands, respectively, and the AM1-BCC atomic charge was calculated using the Antechamber module. The protein-ligand complex was loaded into the leap module, and hydrogen atoms and antagonist ions were automatically added to neutralize the charge. The TIP3P explicit water model was selected and periodic boundary conditions were set. The workflow of molecular dynamics simulation included energy minimization, heating, equilibration and production dynamics. Heavy atoms of proteins (small molecules) were constrained, and water molecules were subjected to 10,000 steps of energy minimization (including 5000-step steepest descent method and 5000-step conjugate gradient method). The system was slowly heated to 300 K within 50 ps and equilibrated for 50 ps under the NPT ensemble. Molecular dynamics simulation was conducted on the system under the NPT ensemble for 50 ns (25,000 steps in total) with a time step of 2 fs. The trajectory data were saved every 10 ps, followed by analysis using the CPPTRAJ module. The free energy of binding for ligands and proteins was calculated using the MMPBA.py module.

3. Results

3.1 Information on Potential Active Ingredients and Targets in BZYQD.

With OB ≥ 30% and DL ≥ 0.18 as the screening criteria, 20 ingredients of Huangqi, 7 ingredients of Baizhu, 22 ingredients of Renshen, 92 ingredients of Gancao, 5 ingredients of Chenpi, 20 ingredients of Chaihu, 2 ingredients of Danggui, and 17 ingredients of Shengma were obtained from the TCMSP. After duplicate values were excluded, 150 active ingredients of BZYQD were obtained. Finally, a total of 265 target genes corresponding to the active ingredients were obtained.

3.2 Information on GC target genes and acquisition of "TCM-Disease" intersection targets.

A total of 12136 GC targets were obtained from the GeneCards database. With a score >10 as the screening criterion, a total of 1383 GC targets were retained. Finally, 136 TCM-Disease intersection targets were obtained using Venn diagram online tool (Figure 2).

3.3 Construction of "TCM–Active Ingredient-Target" network.

The targets and active ingredients of BZYQD in GC were imported into Cytoscape to construct a "TCM-Active Ingredient-Target" network (Figure 3). It was found that the top fivecompounds with the highest degree value in BZYQD were quercetin, kaempferol, nobiletin, naringenin, and formononetin, indicating that these fivecompounds might be the effective components of BZYQD in the treatment of GC (Supplementary Table S1).

Figure 3: “TCM-Active Ingredient-Target” network. The nodes in the outer circle represent all the active ingredients of BZYQD in the treatment of GC (orange: Renshen, yellow: Chenpi, blue: Shengma, cyan: Baizhu, pink: Danggui, purple: Chaihu, teal: Huangqi, green: Gancao); the dark orange nodes in the middle represents the targets of BZYQD acting on the GC.

3.4 Construction of PPI Network and Cluster analysis.

The intersection targets were imported into the STRING database for PPI analysis, and the interaction threshold was set to "0.9" and the unconnected nodes were hidden. Then, the PPI analysis results were imported into Cytoscape software to draw a PPI network diagram (Figure 4). The PPI results demonstrated that the top five core target genes in degree value were AKT1 (RAC-alpha serine/threonine-protein kinase, Degree = 45), STAT3 (Signal transducer and activator of transcription 3, Degree = 40), TP53 (Cellular tumor antigen p53, Degree = 40), MAPK1 (Mitogen-activated protein kinase 1, Degree = 39), and MAPK3 (Mitogen-activated protein kinase 3, Degree = 39). The entire network was divided into three different clusters by means of the MCODE plug-in (Figure 5).

3.5 GO enrichment and KEGG pathway enrichment analysis.

GO and KEGG enrichment analysis on the targets of BZYQD in GC were performed through the Metascape platform. The results showed that there were 2208 BP, 77 CC, and 145 MF in the GO enrichment analysis. KEGG pathway enrichment analysis yielded 172 signaling pathways. According to the *P*-value, the top 10 BP, CC, and MF were selected for visualization (Figure 6). The top 20 pathways of KEGG enrichment analysis were visualized using R software to draw a bubble diagram (Figure 7). The apoptosis signaling pathway, PI3K/Akt signaling pathway, proteoglycan in cancer, IL-17 signaling

pathway, TNF signaling pathway, and HIF-1 signaling pathway were mainly involved (Supplementary Table S2).

Figure 7: KEGG pathway enrichment analysis of the targets of BZYQD in GC. Each bubble represents a KEGG pathway on the vertical axis. The size of the bubble represents the number of genes enriched in each KEGG pathway, and the larger the bubble, the more genes in the pathway. The color of each bubble is determined by the *P*-value, and the redder the color of the bubble, the smaller the *P*-value.

3.6 Molecular docking results.

The five compounds (quercetin, kaempferol, nobiletin, naringenin, and formononetin) with the highest degree value were docked with five core target proteins (AKT1, STAT3, TP53, MAPK1, and MAPK3) in the PPI network by using AutoDock software (Supplementary Table S3). The results demonstrated that the key compounds showed good binding activity with the core target proteins, and the best binding energy was MAPK3-naringenin (-8.08 kcal/mol). The molecule formed two hydrogen bonds with the protein amino acid residues Ser74 and Tyr81 at a distance of 2.57 Å. Moreover, it formed a hydrophobic interaction with Gly54, Ile73, Pro75, and Tyr81, followed by MAKP3-formononetin (-7.97 kcal/mol) and MAPK1-kaempferol (-7.92 kcal/mol). The molecular docking diagram is shown in Figure 8.

3.7 Molecular dynamics simulation results.

Based on the binding energy results, molecular dynamics simulation was performed for MAPK3-Naringenin. The Root-mean-square deviation (RMSD), Radius of gyration (Rog), Root-mean-square fluctuation (RMSF) curve, and binding free energy were calculated.

The RMSD curve represents the variations in protein conformation. The results showed that the RMSD fluctuated greatly in the first 30ns and then gradually stabilized, indicating that the protein-ligand complex formed a stable binding conformation.

The Rog curve displays the compactness of the overall protein structure. It could be seen from the results that the radius of gyration was stable, indicating the compact structure of the protein during the kinetic process and the unchanged conformation.

The RMSF curve represents the variations in the conformation of amino acid residues. It could be seen from the results that the C-terminal region of the protein had greater residue flexibility than other regions. Since this region was a loop-based polypeptide chain, it was more flexible. The results of RMSD, Rog, and RMSF are shown in Figure 9.

The trajectory of the RMSD plateau (30-50 ns) was calculated, allowing the calculation of the free energy of binding for ligand-protein interactions based on the MMGBSA equation. The results showed that the binding free energy of MAPK3-Naringenin was -25 kcal/mol (Supplementary Table S4). Van der Waals potential (-32 kcal/mol) and electrostatic interaction (-26 kcal/mol) were conducive to the combination of the two, while polar solvation (EGB, 37 kcal/mol) was not conducive to the interaction of the two.

The binding site of MAPK3-Naringenin is a binding site with mixed hydrophobic and hydrophilic properties. Residues forming hydrophobic accumulation with ligands included Leu150, Leu101, etc., and residues forming electrostatic interaction included Lys48, Asp161, etc. Hydrophobic accumulation and electrostatic interaction (including hydrogen bonding) were crucial for stable ligand binding. The MAPK3-Naringenin interaction diagram is shown in Figure 10.

Figure 9: Molecular dynamics simulation results for MAPK3-Naringenin.(A) RMSD diagram ; (B) Rog diagram ; (C)

RMSFdiagram.

Figure 10: Residues involved in interactions in the MAPK3-Naringenin.

(A) 3D diagram of ligand-receptor interaction; (B) 2D diagram of ligand-receptor interaction.

4. Discussion

Through the network pharmacological method, this study elucidated that quercetin, kaempferol, nobiletin, naringenin, and formononetin were the active ingredients of BZYQD in the treatment of GC. Prior studies have shown that quercetin can regulate the PI3K/Akt pathway by affecting AKT phosphorylation, down-regulating AKT kinase, and inhibiting EMT in GC cells, thereby repressing GC cell migration and invasion[22–23]. Kaempferol can promote autophagy of GC cells, increase the conversion from LC3-I to LC3-II, and down-regulate the expression of p62 protein in GC[24]. Nobiletin triggers endoplasmic reticulum stress-mediated apoptosis and autophagy of GC cells via the downregulation of the Akt/mTOR signaling[25]. Naringenin can inhibit the proliferation, migration, and invasion of GC cells, and induce apoptosis by inhibiting the phosphorylation of AKT and decreasing the expressions of its downstream target molecules[26]. Formononetin can depress the growth and migration of GC cells by regulating the Wnt/β-Catenin and AKT/mTOR pathways[27].

The results of PPI analysis showed that the targets of BZYQD relating to the treatment of GC mainly involved AKT1, STAT3, TP53, MAPK1, and MAPK3. Akt is a protein kinase that regulates the cell cycle and apoptosis. Activated Akt can interact with several key downstream effectors and phosphorylate, thereby suppressing cell apoptosis[28]. STAT3, a transcription factor of the JAK-STAT signaling pathway, has the ability to promote GC cell proliferation, invasion, and migration[29]. In the tumor microenvironment, tumor cells can secrete interleukin, which in turn activates the STAT3 signaling pathway, leading to the progression and deterioration of GC cells[30]. TP53 is commonly accepted as a tumor suppressor gene. The expression of TP53 is increased continuously during the deterioration of normal gastric mucosa into intestinal metaplasia and then into GC, and TP53 mutation can be frequently observed in GC patients[31]. MAPK is widely implicated in numerous vital biological processes such as cell proliferation, differentiation, and apoptosis through phosphorylation of nuclear transcription factors and related enzymes[32]. MAPK1 activation is indicative of the invasiveness of GC. Down-regulation of MAPK1

expression can retard GC cell growth, promote apoptosis, and suppress migration and invasion[33]. Kim et al.[34] have revealed that MAPK3 expression can be regarded as an independent prognostic index for GC patients receiving resection treatment.

GO enrichment analysis indicated that BZYQD treated GC through a variety of pivotal biological processes such as oxidative stress, chemical stress, lipopolysaccharide reaction, and apoptosis. KEGG pathway enrichment analysis exhibited that the main pathways of BZYQD in the treatment of GC included the apoptosis signaling pathway, PI3K/Akt signaling pathway, proteoglycan in cancer, IL-17 signaling pathway, TNF signaling pathway, and HIF-1 signaling pathway. Among these signaling pathways, apoptosis is undoubtedly highlighted as the most critical signaling pathway in malignant tumors, so the induction of tumor cell apoptosis has emerged as a research hotspot in the treatment of GC[35]. The PI3K/Akt signaling pathway is proposed to be a carcinogenic signaling pathway, which participates in the modulation of diverse biological processes of cancer cells, such as proliferation, apoptosis, chemotherapy resistance, and metastasis[36]. Lee et al.[37] have clarified that inhibition of the PI3K/Akt signaling pathway can lead to G2/M phase arrest, autophagy, and apoptosis of GC cells. Proteoglycan, an important part of extracellular matrix proteins, can mediate the migration and proliferation of tumor cells[38]. The IL-17 signaling pathway can dramatically alter the tumor microenvironment by enhancing the secretion of chemokines and cytokines, thereby promoting tumor occurrence and development[39]. The TNF signaling pathway regulates inflammatory responses in the body. Excessive TNF inflammatory cytokines in the tumor microenvironment can elicit tumor growth and destroy the innate immune response of tumor cells[40]. The HIF-1α signaling is regarded as an initiator of GC progression, which can promote GC cell proliferation and angiogenesis, induce EMT, and enhance the invasion and metastasis of GC, and consequently, inhibition of the HIF-1α signaling can be a promising strategy to prevent GC cells from infiltration and metastasis[41].

5. Conclusion

Through network pharmacology, we revealed the significant advantages of BZYQD in the treatment of GC. BZYQD mainly acts on multiple target genes such as AKT1, STAT3, TP53, MAPK1, and MAPK3 through a variety of compounds including quercetin, kaempferol, nobiletin, naringenin, and formononetin, then interferes with the apoptosis signaling pathway, PI3K/Akt signaling pathway, proteoglycan in cancer, IL-17 signaling pathway, TNF signaling pathway, and HIF-1 signaling pathway, and eventually exerts a therapeutic effect on GC.

Declarations

Acknowledgments

This study was supported by the Science and Technology Research Project of Educational Commission of Hubei Province (Project no. D20172006).

Authors' contributions

Ruiping Yang was responsible for the design, data collection and manuscript of this study. Ruixue Jiang and Chunhui Tao were responsible for the analysis and interpretation of data. Xiaojing Lin was responsible for the visualization of the data. All authors read and approved the final version of the manuscript.

Competing interests

The authors declare no competing interests.

Additional information

Table S1: Top 10 basic information of ingredients in BZYQD by their degree values. Table S2: Information of Top 20 of signaling pathways. Table S3: Molecular docking results of key compounds and core target proteins. Table S4: Binding free energy for MAPK3-Naringenin.

Correspondence and requests for materials should be addressed to R.J.

References

[1] Hyuna Sung, Jacques Ferlay, Rebecca L Siegel R, Mathieu Laversanne M et al. Global Cancer Statistics 2020: GLOBOCAN Estimates of Incidence and Mortality Worldwide for 36 Cancers in 185 Countries. ***CA: A Cancer Journal for Clinicians***. 2021;71:209-249.

[2] Prashanth Rawla and Adam Barsouk. Epidemiology of gastric cancer: global trends, risk factors and prevention. ***Prz Gastroenterol***. 2019;14:26-38.

[3] Mitsuru Sasako. Surgery and adjuvant chemotherapy. ***International Journal of Clinical Oncology***. 2008;13:193-195.

[4] Ebrahim Salehifar, Razieh Avan, Ghasem Janbabaei, Seyed Khalil Mousavi et.al. Comparison the Incidence and Severity of Side Effects Profile Of FOLFOX and DCF Regimens in Gastric Cancer Patients. ***Iranian Journal of Pharmaceutical Research***. 2019;18:1032-1039.

[5] Zhixue Wang, Fanghua Qi, Yangang Cui, Lin Zhao et al. An update on Chinese herbal medicines as adjuvant treatment of anticancer therapeutics. ***BioScience Trends***. 2018;12:220-239.

[6] Te-Hsin Chao, Pin-Kuei Fu, Chiung-Hung Chang, Shih-Ni Chang et al. Prescription patterns of Chinese herbal products for post-surgery colon cancer patients in Taiwan. ***Journal of Ethnopharmacol***. 2014;155:702-8.

[7] Ruihan Xu, Jian Wu, Xingxing Zhang, Xi Zou et al. Modified Bu-zhong-yi-qi decoction synergies with 5 fluorouracile to inhibits gastric cancer progress via PD-1/PD- L1-dependent T cell immunization.

Pharmacological Research. 2020;152:104623.

[8] Ning Yu, Ying Xiong and Chun Wang. Bu-Zhong-Yi-Qi Decoction, the Water Extract of Chinese Traditional Herbal Medicine, Enhances Cisplatin Cytotoxicity in A549/DDP Cells through Induction of Apoptosis and Autophagy. ***BioMed Research International***. 2017, Article ID 3692797, 9 pages.

[9] J. W. Pei, T. Z. Sun, B. F. Fu and S. Q. Jiang. Effects of Buzhong Yiqi Decoction on Th1, Th2 cytokines and Th1/Th2 immune balance in patients with gastric cancer. ***China Journal of Traditional Chinese Medicine and Pharmacy***. 2020;35:3160-3163.

[10] Youzi Dong, Quanlin Zhao and Yuguo Wang. Network pharmacology-based investigation of potential targets of astragalus membranaceous-angelica sinensis compound acting on diabetic nephropathy. ***Scientific reports.*** 2020;11:19496.

[11] Jingyuan Zhang, Xinkui Liu, Wei Zhou, Guoliang Cheng et al. A bioinformatics investigation into molecular mechanism of Yinzhihuang granules for treating hepatitis B by network pharmacology and molecular docking verification. ***Scientific reports***. 2020;10:11448.

[12] Jinlong Ru, Peng Li, Jinan Wang, Wei Zhou et al. TCMSP: a database of systems pharmacology for drug discovery from herbal medicines. ***Journal of Cheminformatics***. 2014;6:13.

[13] Sangya Pundir, Maria Martin and Claire O'Donovan. UniProt Protein Knowledgebase. ***Methods in Molecular Biology***, 2017;1558:41-55.

[14] Marilyn Safran, Irina Dalah, Justin Alexander, Naomi Rosen et al. GeneCards Version 3: the human gene integrator. ***Database***. 2010;baq020.

[15] David Otasek, John H morris, Jorge Boucas, Alexander R Pico et al. Cytoscape Automation: empowering workflow-based network analysis. ***Genome Biology***. 2019;20:185.

[16] Damian Szklarczyk, Annika L Gable, David Lyon, Alexander Junge et al. STRING v11: protein-protein association networks with increased coverage, supporting functional discovery in genome-wide experimental datasets," ***Nucleic Acids Research***. 2019;47:D607-613.

[17] Hasin A Ahmed, Dhruba K Bhattacharyya and Jugal K Kalita. Core and peripheral connectivity based cluster analysis over PPI network. ***Computational Biology and Chemistry***. 2015;58:32-41.

[18] Yingyao Zhou, Bin Zhou, Lars Pache, Max Chang et al. Metascape provides a biologist-oriented resource for the analysis of systems-level datasets. ***NAT COMMUN***. 2019;10;1523.

[19] Sunghwan Kim, Paul A Thiessen, Evan E Bolton, Jie Chen et al. PubChem Substance and Compound databases. ***Nucleic Acids Research***. 2016;44:D1202-13.

[20] Stephen K Burley, Helen M Berman, Charmi Bhikadiya, Chunxiao Bi et al. RCSB Protein Data Bank: biological macromolecular structures enabling research and education in fundamental biology, biomedicine, biotechnology and energy. ***Nucleic Acids Research***. 2019;47:D464-474.

[21] Tai-Sung Lee, David S Cerutti, Dan Mermelstein, Charles Lin. GPU-Accelerated Molecular Dynamics and Free Energy Methods in Amber18: Performance Enhancements and New Features. ***Journal of Chemical Information and Modeling***. 2018;58:2043-2050.

[22] Atousa Haghi, Haniye Azimi and Roja Rahimi. A Comprehensive Review on Pharmacotherapeutics of Three Phytochemicals, Curcumin, Quercetin, and Allicin, in the Treatment of Gastric Cancer. ***Journal of Gastrointestinal Cancer***. 2017;48:314-320.

[23] X. F. Jia, W. M. Chen, D. P. Sun, H. B. Zhao et al. Quercetin in inhibiting the epithelial-mesenchymal transition of gastric cancer. ***Journal of Hainan Medical University***. 2015; 21:1030-1032.

[24] Tae Woo Kim, Seon Young Lee, Mia Kim, Chunhoo Cheon et al. Kaempferol induces autophagic cell death via IRE1-JNK-CHOP pathway and inhibition of G9a in gastric cancer cells. ***Cell Death & Disease***. 2018;9:875.

[25] Jeong Yong Moon and Somi Kim Cho. Nobiletin Induces Protective Autophagy Accompanied by ER-Stress Mediated Apoptosis in Human Gastric Cancer SNU-16 Cells. ***Molecules***. 2016;21:914.

[26] Lei Bao, Feng Liu, Huai-Bin Guo, Yong Li et al. Naringenin inhibits proliferation, migration, and invasion as well as induces apoptosis of gastric cancer SGC7901 cell line by downregulation of AKT pathway. ***Tumour Biology***. 2016;37:11365-74.

[27] Jian-Ning Yao, Xue-Xiu Zhang, Yan-Zhen Zhang, Jia-Heng Li et al. Discovery and anticancer evaluation of a formononetin derivative against gastric cancer SGC7901 cells. ***Investigational New Drugs***. 2019;37:1300-1308.

[28] Eiji Oki, Hideo Baba, Eriko Tokunaga, Toshihiko Nakamura et al. Akt phosphorylation associates with LOH of PTEN and leads to chemoresistance for gastric cancer. ***International Journal of Cancer***. 2005;117:376-380.

[29] Jie Yuan, Fei Zhang and Ruifang Niu. Multiple regulation pathways and pivotal biological functions of STAT3 in cancer. ***Scientific Reports***. 2015;5:17663.

[30] Milad Ashrafizadeh, Ali Zarrabi, Sima Orouei, Vahideh Zarrin et al. STAT3 Pathway in Gastric Cancer: Signaling, Therapeutic Targeting and Future Prospects. ***Biology***. 2020;9:126.

[31] Rita A Busuttil, Giada V Zapparoli, Sue Haupt, Christina Fennell et al. Role of p53 in the progression of gastric cancer. ***Oncotarget***. 2014;5:12016-12026.

[32] Lyn M Wancket, W Joshua Frazier and Yusen Liu. Mitogen-activated protein kinase phosphatase (MKP)-1 in immunology, physiology, and disease. ***Life Sciences***. 2012;90:237-48.

[33] Bojian Fei and Haorong Wu. MiR-378 inhibits progression of human gastric cancer MGC-803 cells by targeting MAPK1 in vitro. ***Oncology Research***. 2012;20:557-64.

[34] Jong Gwang Kim, Soo Jung Lee, Yee Soo Chae, Byung Woog Kang et al. Association between phosphorylated AMP-activated protein kinase and MAPK3/1 expression and prognosis for patients with gastric cancer. ***Oncology***. 2013;85:78-85.

[35] Jun-Rong Liang and Hui Yang. Ginkgolic acid (GA) suppresses gastric cancer growth by inducing apoptosis and suppressing STAT3/JAK2 signaling regulated by ROS. ***Biomedicine & pharmacotherapy***. 2020;125:109585.

[36] Sadegh Fattahi, Fatemeh Amjadi-Moheb, Reza Tabaripour, Gholam Hossein Ashrafi et al. PI3K/AKT/mTOR signaling in gastric cancer: Epigenetics and beyond. ***Life Sciences***. 2020;262:118513.

[37] Ho Jeong Lee, Venu Venkatarame Gowda Saralamma, Seong Min Kim, Sang Eun Ha et al. Pectolinarigenin Induced Cell Cycle Arrest, Autophagy, and Apoptosis in Gastric Cancer Cell via PI3K/AKT/mTOR Signaling Pathway. ***Nutrients***. 2018;10:1043.

[38] Rosetta Merline, Roland M Schaefer and Liliana Schaefer. The matricellular functions of small leucine-rich proteoglycans (SLRPs). ***Journal of Cell Communication and Signaling***. 2009;3:323-35.

[39] Jérémy Bastid, Cécile Dejou, Aurélie Docquier and Nathalie Bonnefoy. The Emerging Role of the IL-17B/IL-17RB Pathway in Cancer. ***Frontiers in Immunology***. 2020;11:718.

[40] Xueqiang Zhao, Lijie Rong, Xiaopu Zhao, Xiao Li et al. TNF signaling drives myeloid-derived suppressor cell accumulation. ***Journal of Clinical Investigation***. 2012;122:4094-104.

[41] Hongyu Li, Yanfei Jia and Yunshan Wang. Targeting HIF-1α signaling pathway for gastric cancer treatment. ***Die Pharmazie***. 2019;74:3-7.

Tables

Due to technical limitations, table 1, 2, 3 and 4 is only available as a download in the Supplemental Files section.

Figures

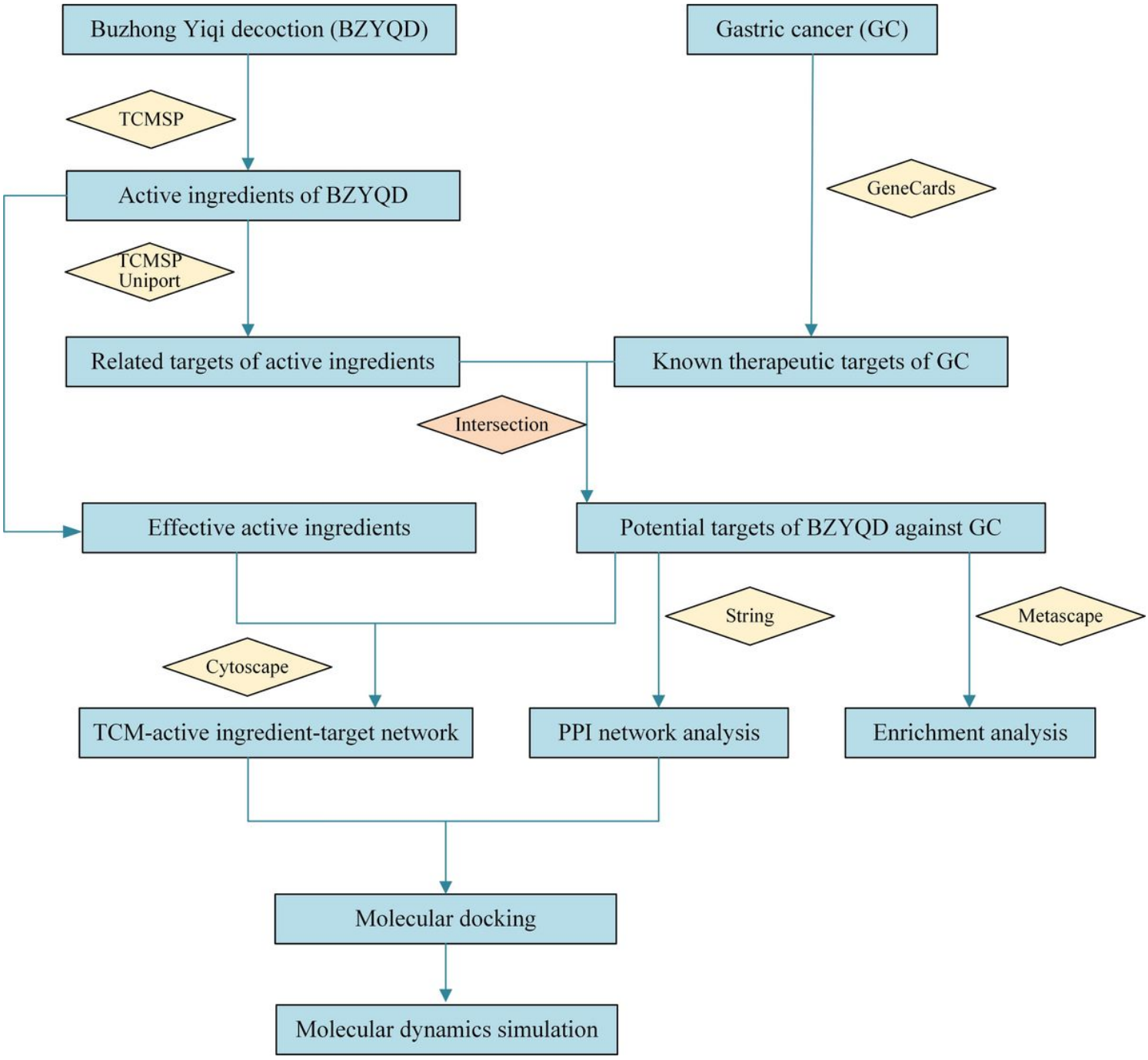

Figure 1

The detailed flowchart of the present study.

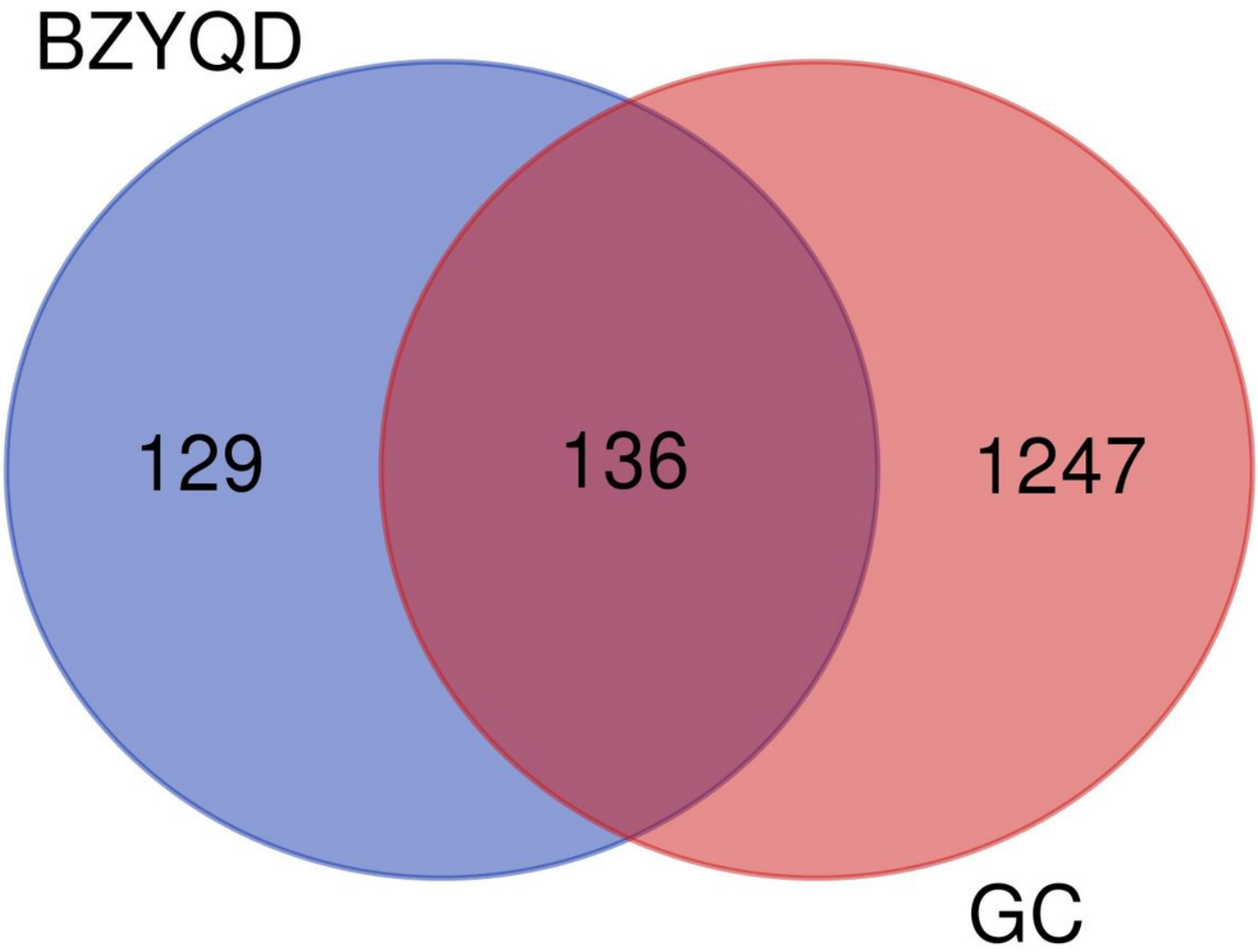

Figure 2

Venn diagram of intersection between BZYQD (blue) and GC (red) targets.

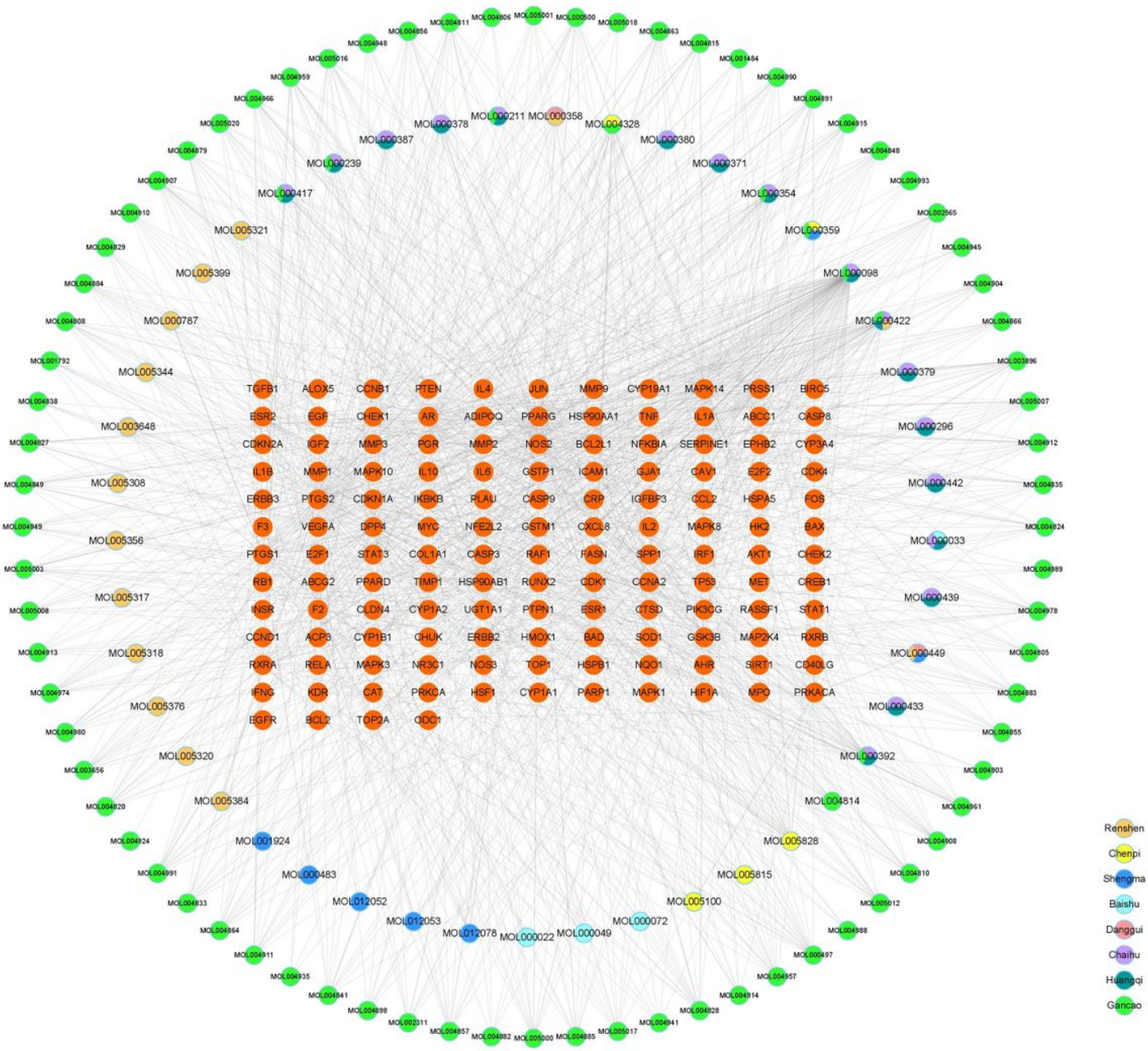

Figure 3

“TCM-Active Ingredient-Target” network. The nodes in the outer circle represent all the active ingredients of BZYQD in the treatment of GC (orange: Renshen, yellow: Chenpi, blue: Shengma, cyan: Baizhu, pink: Danggui, purple: Chaihu, teal: Huangqi, green: Gancao); the dark orange nodes in the middle represents the targets of BZYQD acting on the GC.

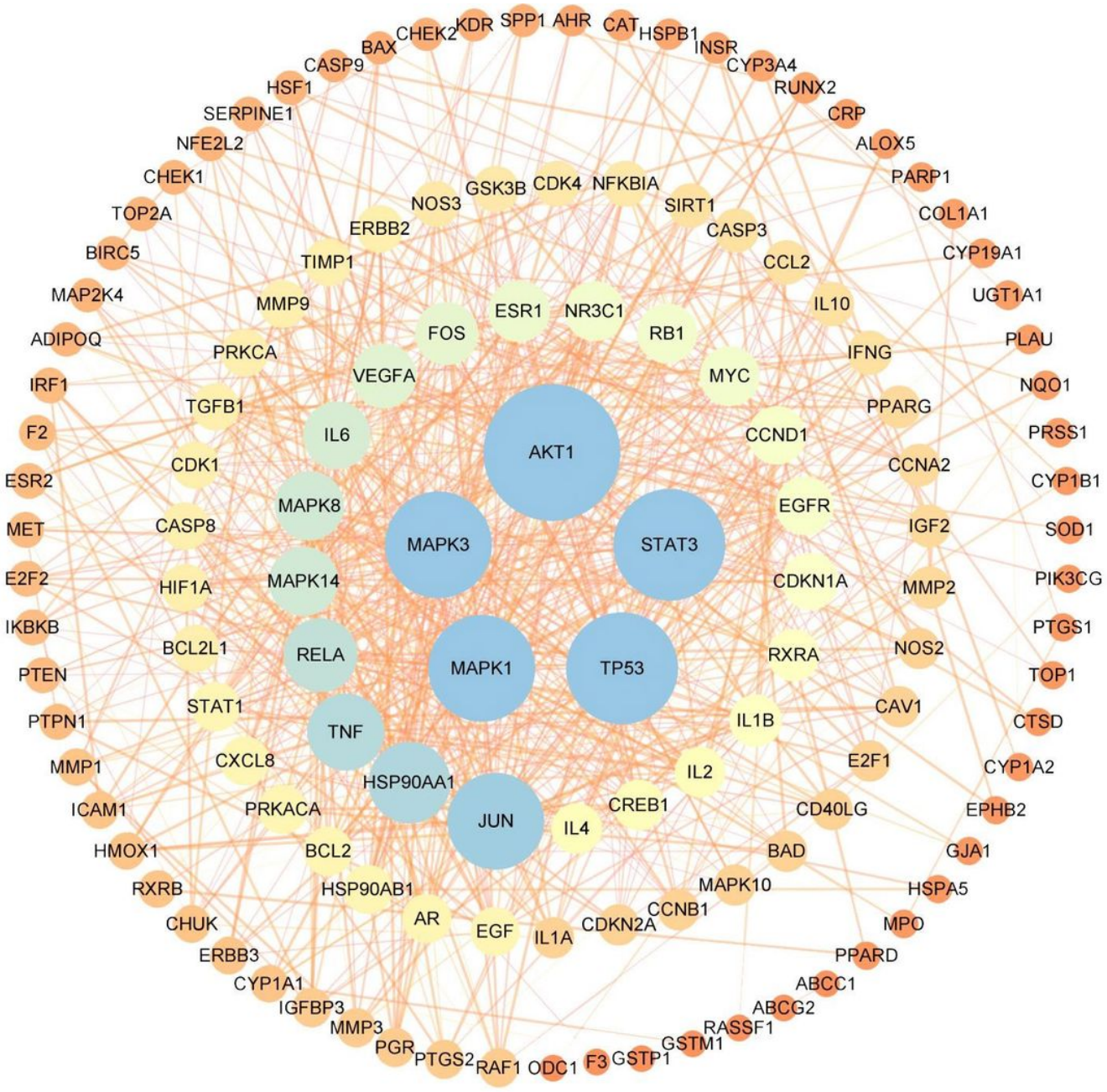

Figure 4

The protein-protein interaction network. The sizes and colors of the nodes and edges are illustrated from big to small and blue to orange in descending order of degree values.

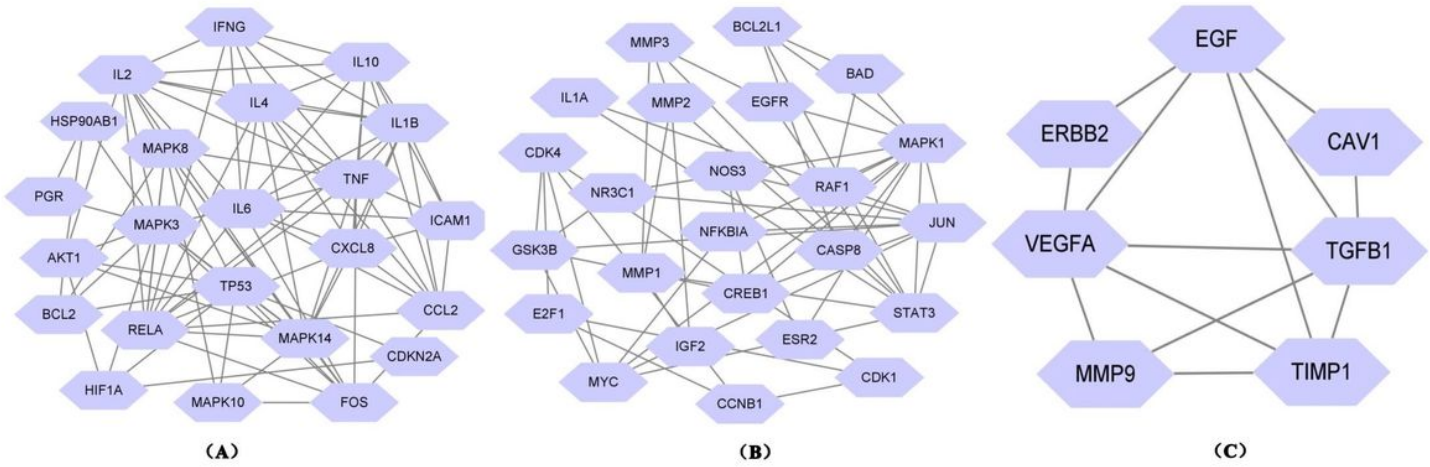

Figure 5

Mcode clustering in the protein-protein interaction network. A-C represent clusters 1, 2, and 3, respectively.

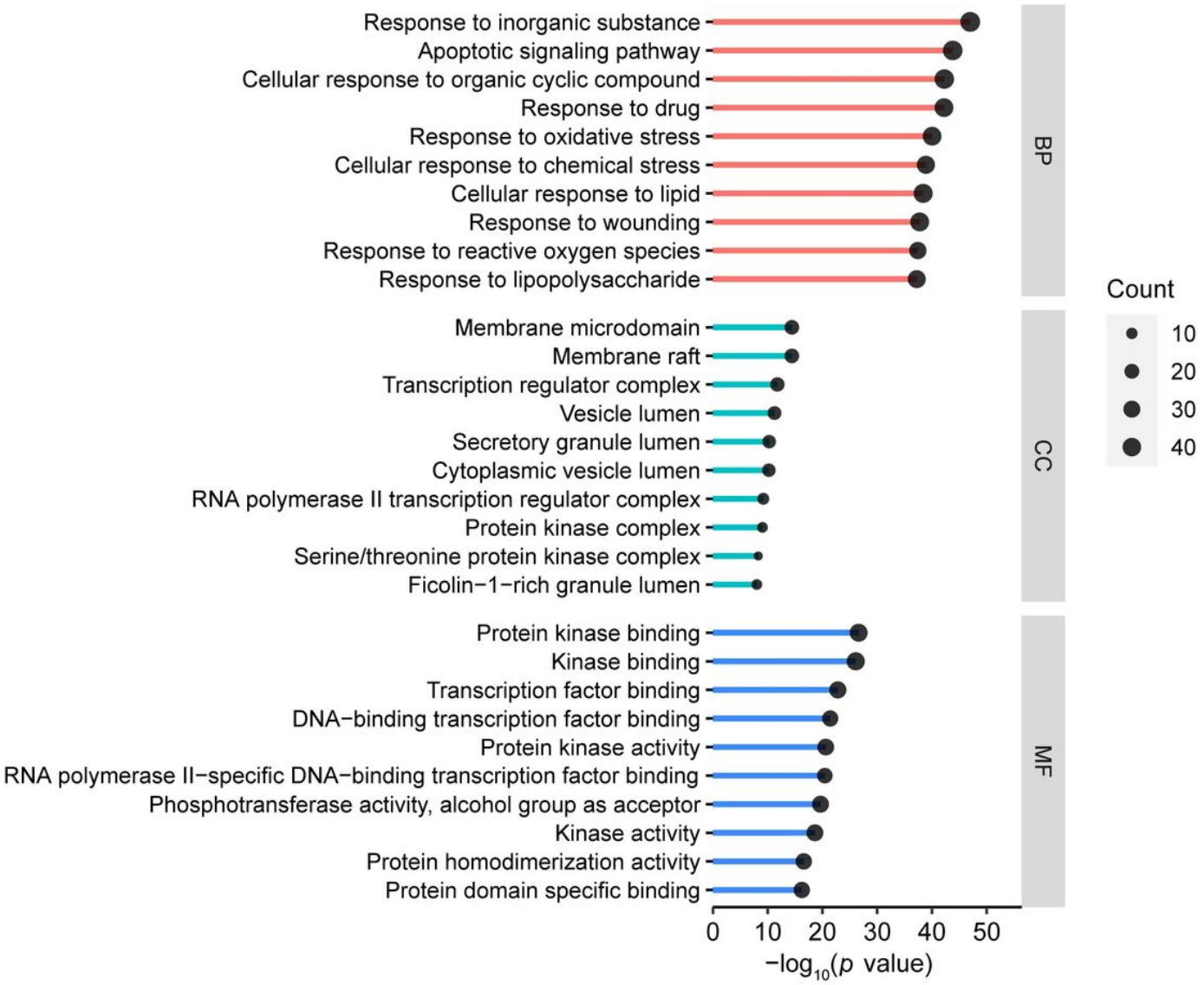

Figure 6

GO functional enrichment analysis of the targets of BZYQD in GC. Each bar indicates a GO term on the vertical axis. The bubble in the bar represents the number of genes enriched in each GO term. The larger the bubble, the more genes in the GO term. The length of each bar is determined by the P-value. The longer the bar, the smaller the P-value.

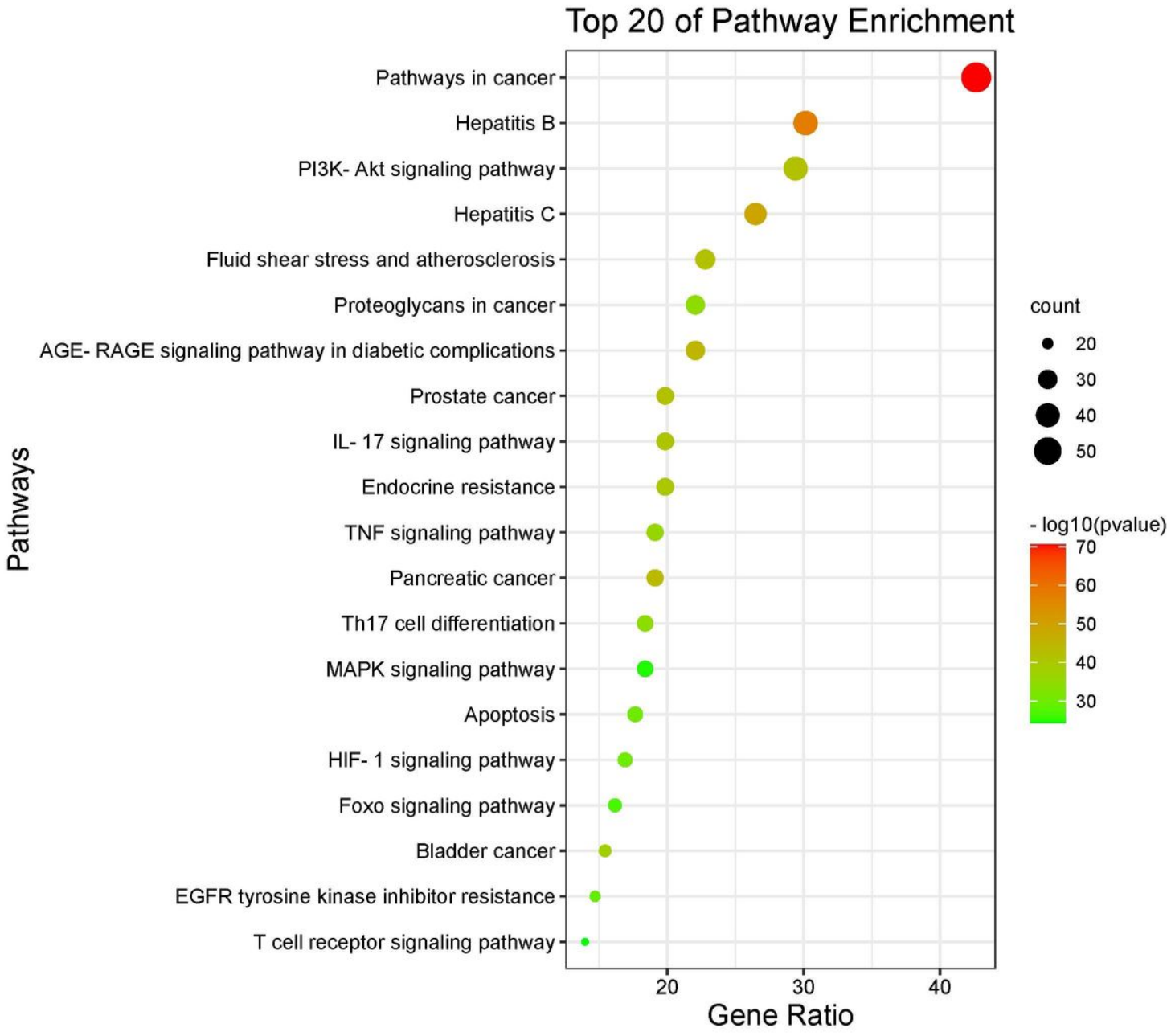

Figure 7

KEGG pathway enrichment analysis of the targets of BZYQD in GC. Each bubble represents a KEGG pathway on the vertical axis. The size of the bubble represents the number of genes enriched in each KEGG pathway, and the larger the bubble, the more genes in the pathway. The color of each bubble is determined by the P-value, and the redder the color of the bubble, the smaller the P-value.

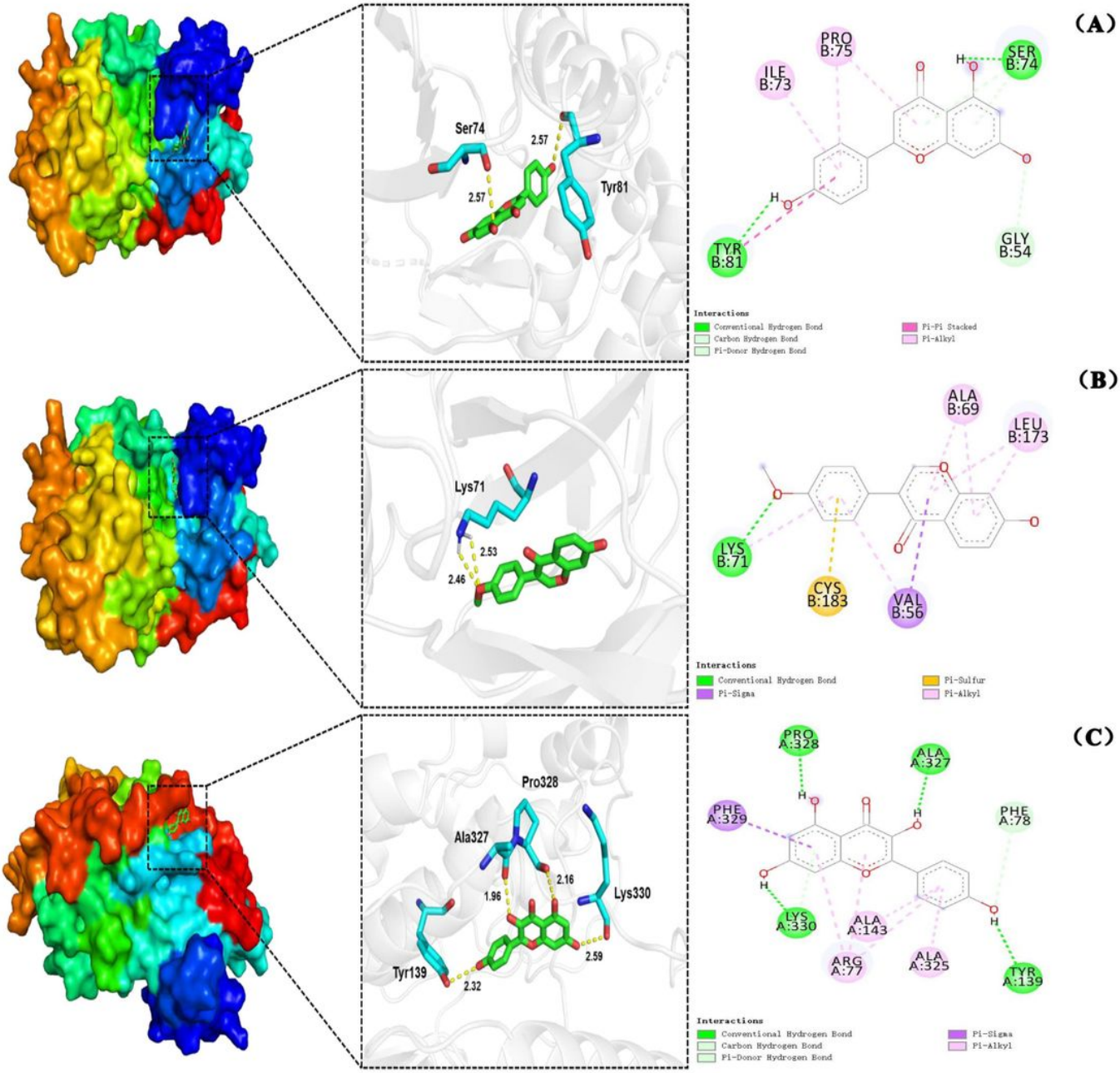

Figure 8

Molecular docking diagram. (A) Naringenin-MAPK3, (B) Formononetin-MAPK3, (C) Kaempferol-MAPK1.

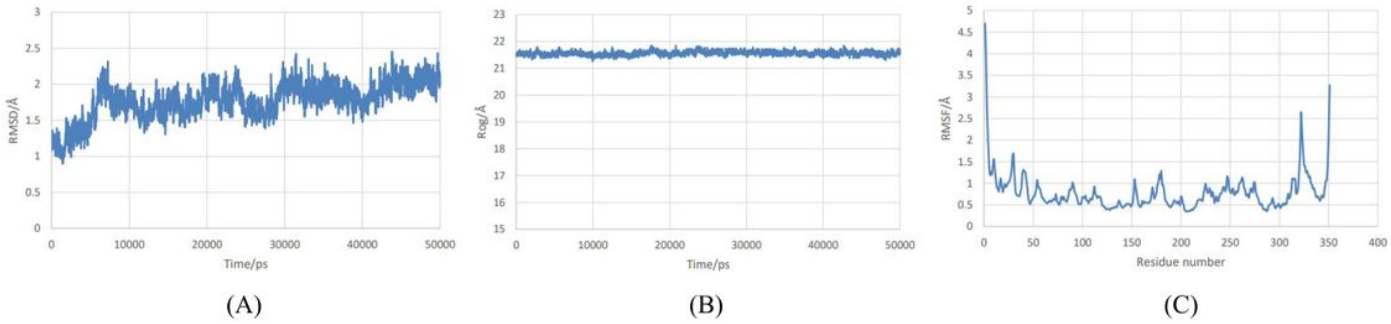

Figure 9

Molecular dynamics simulation results for MAPK3-Naringenin. (A) RMSD diagram ; (B) Rog diagram ; (C) RMSF diagram.

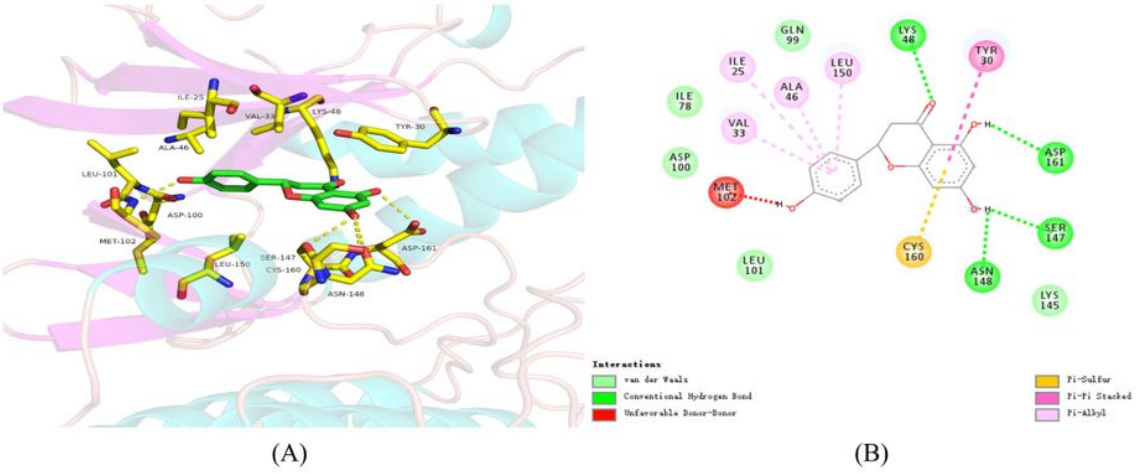

Figure 10

Residues involved in interactions in the MAPK3-Naringenin. (A) 3D diagram of ligand-receptor interaction; (B) 2D diagram of ligand-receptor interaction.

Supplementary Files

This is a list of supplementary files associated with this preprint. Click to download.

- Table1.Top10basicinformationofingredientsinBZYQDbytheirdegreevalues.xlsx
- Table2.InformationofTop20ofsignalingpathways.xlsx
- Table3.Moleculardockingresultsofkeycompoundsandcoretargetproteins.xlsx

- Table4.BindingfreeenergyforMAPK3Naringenin.xlsx